Title

The activities of LDL Receptor-related Protein-1 (LRP1) compartmentalize into distinct plasma membrane microdomains

Permalink

https://escholarship.org/uc/item/65d5b139

Authors

Laudati, Emilia
Gilder, Andrew S
Lam, Michael S
et al.

Publication Date

2016-10-01

DOI

10.1016/j.mcn.2016.08.006

HHS Public Access

The activities of LDL Receptor-related Protein-1 (LRP1) compartmentalize into distinct plasma membrane microdomains

Emilia Laudati[1,2], **Andrew S. Gilder**[1], **Michael S. Lam**[1], **Roberta Misasi**[3], **Maurizio Sorice**[3], **Steven L. Gonias**[1], and **Elisabetta Mantuano**[1,3,*]

[1]Department of Pathology, University of California San Diego, La Jolla CA, USA.

[2]Institute of Pharmacology, Catholic University Medical School, Rome, Italy.

[3]Department of Experimental Medicine, Sapienza University of Rome, Rome, Italy.

Abstract

LDL Receptor-related Protein-1 (LRP1) is an endocytic receptor for diverse ligands. In neurons and neuron-like cells, ligand-binding to LRP1 initiates cell-signaling. Herein, we show that in PC12 and N2a neuron-like cells, LRP1 distributes into lipid rafts and non-raft plasma membrane fractions. When lipid rafts were disrupted, using methyl-β-cyclodextrin or fumonisin B1, activation of Src family kinases and ERK1/2 by the LRP1 ligands, tissue-type plasminogen activator and activated α_2-macroglobulin, was blocked. Biological consequences of activated LRP1 signaling, including neurite outgrowth and cell growth, also were blocked. The effects of lipid raft disruption on ERK1/2 activation and neurite outgrowth, in response to LRP1 ligands, were reproduced in experiments with cerebellar granule neurons in primary culture. Because the reagents used to disrupt lipid rafts may have effects on the composition of the plasma membrane outside lipid rafts, we studied the effects of these reagents on LRP1 activities unrelated to cell-signaling. Lipid raft disruption did not affect the total ligand binding capacity of LRP1, the affinity of LRP1 for its ligands, or its endocytic activity. These results demonstrate that well described activities of LRP1 require localization of this receptor to distinct plasma membrane microdomains.

Keywords

LDL Receptor-related Protein-1 (LRP1); lipid rafts; cell signaling; neurite outgrowth; plasma membrane; Tissue plasminogen activator (tPA); endocytosis

1. Introduction

Compared with the original fluid mosaic model of plasma membrane structure (Singer and Nicolson, 1972), it is now accepted that the molecular composition of the plasma membrane

*To whom correspondence should be addressed: Elisabetta Mantuano, Department of Pathology, University of California San Diego School of Medicine, 9500 Gilman Drive, La Jolla CA, 92093-0612, USA. Tel: (858) 534-1887; Fax: (858) 534-0414; emantuano@ucsd.edu.

is heterogeneous (Brown and London, 1998). Specialized plasma membrane microdomains facilitate important membrane activities. Lipid rafts, which are sphingolipid and cholesterol-enriched microdomains, impose an increased degree of rigidity on the plasma membrane and play an essential role in assembling protein complexes involved in cell-signaling (Brown and London, 1998, 2000; Simons and Toomre, 2000). In neurons, lipid rafts function in axonal development and maintenance of synaptic integrity (Allen et al., 2007; Hering et al., 2003). Furthermore, lipid rafts have been implicated in the pathogenesis of several neurodegenerative diseases including Alzheimer's disease (AD) (Cordy et al., 2006; Liu et al., 2007; Simons and Ehehalt, 2002).

LDL Receptor-related Protein-1 (LRP1) is a type 1 transmembrane protein and member of the LDL Receptor (LDL-R) gene family, implicated in endocytosis, phagocytosis, efferocytosis, and cell-signaling (Gonias and Campana, 2014; Herz and Strickland, 2001). LRP1 ligands are numerous and structurally diverse. The LDL-R, by contrast, has a more limited repertoire of ligands and functions in the internalization of cholesterol-rich LDL (Goldstein et al., 1985). Early studies demonstrated that the LDLR is localized mainly in clathrin-coated pits, which occupy about 2% of the plasma membrane surface (Goldstein et al., 1979). We demonstrated, using immuno-electron microscopy, that in vascular smooth muscle cells (VSMCs), LRP1 is localized almost entirely in coated pits (Weaver et al., 1996). The cytoplasmic tail of LRP1 includes motifs that may serve as coated pit endocytosis signals, including NPxY, YxxL, and a dileucine motif (Li et al., 2000).

Boucher et al. (Boucher et al., 2002) first demonstrated that LRP1 may localize within caveolae, a specialized form of lipid raft. These investigators also demonstrated that, in response to PDGF receptor (PDGFβR) activation, the LRP1 intracellular light chain becomes phosphorylated selectively in caveolae. This is important because LRP1 light chain phosphorylation may be an essential upstream event in LRP1 signaling (Herz and Strickland, 2001). Thrombospondin-induced focal adhesion disassembly, a process that may require LRP1-iniated cell-signaling, depends on intact lipid rafts (Barker et al., 2004; Wang et al., 2014). In myocardium, sorting of LRP1 into lipid rafts and the contribution of LRP1 to ERK1/2 activation may depend on whether the cardiomyocytes are normal or stressed (Roura et al., 2014).

Based on a comparison of different cell lines, we previously proposed that LRP1 partitions into both lipid raft and non-raft membrane fractions and the degree to which LRP1 localizes in rafts is cell type-specific (Wu and Gonias, 2005). Interestingly, the activity of LRP1 in cell-signaling also appears to be cell type-specific (Gonias and Campana, 2014). In neurons, LRP1-activated cell-signaling has been implicated in neuronal survival (Fuentealba et al., 2009; Hayashi et al., 2007), neurite outgrowth (Mantuano et al., 2008; Matsuo et al., 2011; Qiu et al., 2004; Shi et al., 2009), growth cone navigation (Landowski et al., 2016), synaptic transmission (May et al., 2004), and long-term potentiation (Zhuo et al., 2000). In cerebellar granule neurons (CGNs) and neuron-like cell lines, activation of cell-signaling proteins downstream of LRP1, including Src family members (SFKs), ERK1/2, Akt, and RhoA, depends on the assembly of systems of co-receptors that include the NMDA Receptor, Trk receptors, and/or p75 [NTR] (Mantuano et al., 2013; Mantuano et al., 2008; Shi et al., 2009).

In this study, we examined the role of lipid rafts in the function of LRP1 in neurons and neuron-like cells. We find that disrupting lipid rafts entirely blocks cell-signaling triggered by LRP1 ligands, including tissue-type plasminogen activator (tPA) and activated α_2-macroglobulin (α_2M*). Loss of LRP1 signaling activity neutralized the ability of LRP1 to regulate neurite outgrowth and cell growth. The reagents used to disrupt lipid rafts had no effects on the ligand-binding capacity of LRP1, its affinity for ligands, or the function of LRP1 in endocytosis, activities presumed to be localized to clathrin-coated pits and not lipid rafts. Distribution of LRP1 into more than one plasma membrane microdomain provides a mechanism by which distinct activities of this multifunctional receptor may be independently regulated.

2. Materials and Methods

2.1. Proteins and reagents

Enzymatically-inactive tPA (EI-tPA), which is mutated at S478A and R275E and thus, inactive and non-cleavable was purchased from Molecular Innovations (Novi, MI). We confirmed that EI-tPA is inactive by measuring the rate of hydrolysis of H-D-isoleucyl-L-prolyl-L-arginine p-nitroanilide 2HCl (S-2288, Chromogenix, Bedford, MA). α_2M was purified from human plasma by the method of Imber and Pizzo (Imber and Pizzo, 1981) and activated to form α_2M* by treatment with 200 mM methylamine in 50 mM Tris-HCl, pH 8.2 for 6 h. Unreacted methylamine was removed by extensive dialysis against 20 mM sodium phosphate, 150 mM NaCl, pH 7.4 (PBS) (Hussaini et al., 1990; LaMarre et al., 1993). Modification of α_2M by methylamine was confirmed by the characteristic increase in α_2M electrophoretic mobility by nondenaturing PAGE (Imber and Pizzo, 1981). α_2M* and EI-tPA were sterile-filtered using 0.22-μm syringe microfilters and used within 2 wks. The LRP1 ligand-binding antagonist, Receptor-associated Protein (RAP), was expressed as a Glutathione S-transferase (GST) fusion protein in bacteria and purified as previously described (Webb et al., 1995). RAP was subjected to chromatography on Detoxi-Gel endotoxin-removing columns (Pierce). For immuno-blotting experiments, we used an antibody that detects the LRP1 85-kDa β-chain (Sigma). Rabbit polyclonal antibodies that detect phospho-ERK1/2, total ERK1/2, and PDGFβR were from Cell Signaling Technologies (Danvers, MA). Polyclonal antibody that detects Caveolin was from BD Biosciences. Monoclonal antibody specific for β-actin and polyclonal antibody specific for Calnexin were from Sigma. Horseradish peroxidase-conjugated secondary antibodies were from Cell Signaling Technologies.

2.2 Cell culture

Rat PC12 pheochromocytoma cells were obtained from the ATCC (Catalogue no. CRL-1721) and cultured in Dulbecco's modified Eagle's medium (DMEM, high glucose; Invitrogen) containing 10% FBS (Hyclone), 5% heat-inactivated horse serum (Omega Scientific Inc.), penicillin (100 units/ml), and streptomycin (1 mg/ml). Mouse N2a neuroblastoma cells were a generous gift from Dr. Katerina Akassoglou (Gladstone Institute of Neurological Disease, University of California, San Francisco, CA). N2a cells were cultured in DMEM containing 10% FBS, penicillin, and streptomycin. Primary cultures of CGNs were established using cells isolated from cerebellum of 7-day-old Sprague–Dawley

rat pups as previously described (Shi et al., 2009). In brief, freshly dissected cerebella were dissociated in the presence of trypsin and DNase I. Cells were plated in poly-L-lysine-coated dishes at a density of 1.5×10^6 cells/ml in Neuro-basal Medium supplemented with 10% B-27 supplement, 25 mM KCl, penicillin and streptomycin. Cytosine arabinoside (10 μM) was added to the culture medium 24 h after initial plating.

2.3. Sucrose density gradient ultracentrifugation

Lipid raft-associated proteins were identified by buoyant density in sucrose gradients as previously described (Wu and Gonias, 2005). Briefly, cells were washed three times with PBS, collected by scraping into 25 mM 2-[N-morpholino] ethanesulfonic acid, 150 mM NaCl, pH 6.5 containing 1% Triton X100 and protease inhibitor cocktail, and homogenized by 20 strokes through a 25 gauge needle. Preparations were incubated on ice for 30 min. Following centrifugation at $300 \times g$ for 5 min, supernatants were collected and equilibrated in 2 mL of 45% sucrose and loaded in ultracentrifuge tubes. A discontinuous sucrose gradient was constructed by adding 35% sucrose (2 mL) and 5% sucrose (1 mL) on top of each sample. Ultracentrifugation was conducted at 46,000 rpm for 18 h at 4° in a Beckman 50.1 rotor. Ten 0.5 mL fractions were collected from each centrifuge tube, without disturbing the established gradient. Fractions were analyzed by SDS-PAGE and immunoblotting.

2.4. Analysis of cell-surface proteins by detergent solubility

PC12 and N2a cells (1×10^6 cells/well) were plated in six-well culture dishes (Falcon) and grown until confluent. The cells were washed three times with PBS and then treated with 2.5 mg/ml of EZ-Link Sulfo-NHS-LC-Biotin (ThermoScientific) for 1 h at 4° C to label cell-surface proteins. The cells were washed extensively with PBS and 100 mM glycine for 30 min and then detached by scraping and extracted in 1% Triton X100 containing protease inhibitor cocktail for 30 min at 4° C. Preparations were centrifuged at $12,000 \times g$ for 20 min at 4° C. Supernatants were collected as the Triton X100-soluble fraction. The Triton X100-insoluble pellet was extracted in RIPA buffer. Biotinylated proteins in both fractions were affinity precipitated with Streptavidin-Seph-arose (Amersham Biosciences). Affinity-precipitated proteins and total extracts were analyzed by SDS PAGE and immunoblot analysis.

2.5. Gene silencing

Previously characterized rat LRP1-specific siRNA (CGAGCGACCUCCUAUCUUUUU) (47) and pooled non-targeting control (NTC) siRNA were from Dharmacon. PC12 cells (2×10^6) were transfected with LRP1-specific or NTC siRNA (25 nm) by electroporation using the Cell Line Nucleofector Kit V (Amaxa). Gene silencing were determined by RT-qPCR and immunoblot analysis and was always >90%.

2.6. Analysis of cell-signaling

PC12 and N2a cells were plated in 100 mm dishes at a density of 2×10^6 cells/well in serum-containing medium and cultured until ~70% confluent. The cultures were then transferred into SFM for 4 h before adding $\alpha_2 M^*$, EI-tPA, or vehicle. Some cultures were

pre-treated with 1 mM MβCD (Sigma) for 30 min at 37°C or 25 μM Fumonisin FM (Sigma) for 24 h. RAP (250 nM) was added 30 min before other LRP1 ligands. Incubations with LRP1 agonists were conducted for 10 min unless otherwise stated. The cells were then rinsed twice with ice-cold phosphate-buffered saline (PBS). Cell extracts were prepared in radioimmune precipitation assay buffer (PBS with 1% Triton X-100, 0.5% sodium deoxycholate, 0.1% SDS, protease inhibitor mixture, and sodium orthovanadate). The protein concentration in cell extracts was determined by bicinchoninic acid assay. An equivalent amount of cellular protein (40 μg) was subjected to 8-12% SDS-PAGE. Proteins were transferred to nitrocellulose membranes (Bio-Rad) and probed with monoclonal antibody against phospho-ERK1/2 (Sigma-Aldrich) and total ERK1/2 (Life Technologies). Bound antibodies were visualized with HRP-conjugated anti-rabbit IgG (Sigma-Aldrich), by chemiluminescence using the ECL Western Blotting system (Perkin Elmer). In separate studies, nitrocellulose membranes were probed with antibodies that detect phosphorylated members of the c-Src family and total SFK (Cell Signaling Technologies). All immunoblotting studies were performed at least three times.

2.7. Determination of viable cell count

PC12 cells (10^4) were plated in 96-well plates and cultured in SFM with or without 1 mM MβCD for 24 h at 37°C. Other additions included 10% FBS and α_2M^* (10 nM). Viable cells were quantitated using the WST-1 (2-(2-methoxy-4-nitrophenyl)-3-(4-nitrophenyl)-5-(2,4-disulfophenyl)-2H-tetrazolium) assay, as described by the manufacturer (Cayman).

2.8. Binding isotherms

α_2M^* was radio-iodinated using IODO-BEADS® according to the manufacturer's instructions. The specific activity of ^{125}I-α_2M^* was 1.0-1.5×10^6 cpm/μg. PC12 cells were plated in 24-well plates (2×10^5 cells/well), pre-treated with 1 mM MβCD or vehicle for 30 min, and then equilibrated at 4° C in Earle's balanced salt solution, 10 mM Hepes, and 2 mg/ml BSA, pH 7.4 (EHB medium). Increasing concentrations (0.1-15 nM) of ^{125}I-labeled α_2M^* were added to each well, in the presence or absence of a 100-fold molar excess of unlabeled α_2M^*, and allowed to incubate with gentle agitation at 4° C for 4 h. After extensive washing at 4° C, the cells were solubilized with 1.0 M NaOH/0.1% SDS. Cell-associated radioactivity was determined in a γ-counter. Specific binding was determined as the fraction of radioligand binding that was displaced by unlabeled α_2M^*. Independent binding curves from three replicate experiments were fit to the equation for a rectangular hyperbolae using GraphPad Prism. K_D and B_{max} values are reported as the mean ± SEM (n=3).

2.9. Endocytosis assays

PC12 cells were pre-treated with MβCD or vehicle, washed and then, reequilibrated in EHB medium. ^{125}I-labeled α_2M^* was added to each well in the presence or absence of a 100-fold molar excess of unlabeled α_2M^*. The cells were cultured at 37° C for up to 80 min. Uptake was stopped by rapid washing of the cells with ice-cold PBS. Surface-associated radio-ligand, which was not internalized, was dissociated by a brief wash with low pH buffer (pH 2.5-2.8). Cells were then extracted in NaOH and SDS and cell-associated radioactivity was

determined in a gamma counter. Specific ^{125}I-α_2M* uptake was determined as the fraction of uptake displaced by unlabeled α_2M* and is reported as the mean ± SEM (n=3).

2.10. Neurite outgrowth

PC12 cells were plated at 2×10^5 cells/well and maintained in serum-containing medium for 24 h. The medium then was replaced with SFM supplemented with 1 mM MβCD or vehicle and, in some wells, with 12 nM EI-tPA or 10 nM α_2M*, for 48 h. The cells were imaged by phase contrast microscopy, using a Leica microscope equipped with a DFC 300 digital camera and Open Laboratory software.

CGNs were cultured on glass coverslips. Cells were treated with 12 nM EI-tPA, 10 nM α_2M*, or vehicle, in the presence or absence of 1 mM MβCD for 48 h. The cells were then fixed with 4% paraformaldehyde and immunostained with β3-tubulin-specific antibody. Nuclei were labeled with DAPI. Neurite length was determined in 40-50 neurons using Image J software (NIH). Results were subjected to statistical analysis using GraphPad Prism.

2.11. ERK1/2 phosphorylation in CGNs

CGNs on glass coverslips were pre-treated with 1 mM MβCD or vehicle for 30 min and then with 12 nM of EI-tPA, 10 nM α2M*, or vehicle for 10 min. The cells were washed, fixed in 4% paraformaldehyde, and immunostained to detect phospho-ERK1/2. Preparations were mounted on slides using Pro-Long Gold with DAPI. Images were captured using a Leica fluorescence microscope equipped with a Hamamatsu CCD camera and SimplePCI software.

3. Results

3.1. LRP1 localizes partially to lipid rafts in neuron-like cells

Lipid raft-enriched membrane fractions may be resolved from other plasma membrane fractions based on buoyant density in sucrose gradients (Brown and Rose, 1992; Sargiacomo et al., 1993). Using this approach, we previously demonstrated that LRP1 localization in lipid rafts is cell type-specific (Wu and Gonias, 2005). In this study, we focused on neurons and neuron-like cell lines, given the robust cell-signaling activity of LRP1 in these cells (Mantuano et al., 2013; Shi et al., 2009). To begin, we homogenized PC12 neuron-like cells in 1.0% Triton X100 at 4° C and analyzed the extracts by sucrose gradient ultracentrifugation (Fig. 1A). Lipid raft components are typically recovered in low density fractions. LRP1 was recovered in high-density fractions and in low-density fractions, together with caveolin-1, a scaffolding protein in caveolae and bio-marker of lipid raft-like membrane microdomains (Cohen et al., 2004). Calnexin is an integral membrane protein in the endoplasmic reticulum that may be recovered in low density fractions but, in isolates from most cells, is recovered mainly in high density fractions (Li et al., 2003; Vetrivel et al., 2004; Williamson et al., 2010). In PC12 cells, calnexin was recovered in high density fractions. These results suggest that in PC12 cells, LRP1 localizes at least partially in lipid raft-like membrane microdomains.

Triton X100 homogenates also were prepared from N2a neuron-like cells and subjected to sucrose gradient ultracentrifugation. Fig. 1B shows that in N2a cell homogenates, LRP1 was once again recovered in low density, lipid raft-enriched fractions, together with caveolin-1. Calnexin was restricted to high density fractions. As a control, we examined VSMCs and CHO-K1 cells because we previously demonstrated that LRP1 is largely excluded from lipid rafts in these cells (Wu and Gonias, 2005). Fig. 1C shows that in Triton X100 homogenates from VSMCs, LRP1 was recovered mainly in high density fractions and excluded from lower density fractions that contain lipid raft components. Caveolin was identified in low and high density fractions, confirming that the gradients were effective. Similarly, in isolates from CHO-K1 cells, LRP1 was recovered mainly in high density fractions suggesting exclusion from lipid rafts (Fig. 1D). Interestingly, in VSMC and CHO-K1 cells, a slightly increased amount of calnexin distributed into low density fractions, compared with PC12 and N2a cells.

As a second method to examine LRP1 partitioning into lipid rafts, we compared the solubility of membrane proteins in 1.0% Triton X100 at 4° C, without sucrose gradient ultracentrifugation. We applied a previously described modification of this procedure in which we pre-label cells with a membrane-impermeable biotinylation reagent (Wu and Gonias, 2005). Affinity precipitation of biotinylated proteins in detergent-soluble and - insoluble fractions excludes proteins from organelles other than the plasma membrane from the analysis. Fig. 1E shows that biotinylated LRP1 from PC12 cells partitioned into both the detergent-soluble and –insoluble fractions. The latter includes lipid raft-associated proteins (Wu and Gonias, 2005). As a control, we examined the lipid raft-associated receptor tyrosine kinase, PDGFβR, which partitioned exclusively into the detergent-insoluble fraction, as anticipated. Fig. 1F shows that biotinylated LRP1 from N2a cells also partitioned into detergent-soluble and –insoluble fractions. Once again, in these cells, PDGFβR was recovered only in the detergent-insoluble fraction. These results confirm those obtained using sucrose density ultracentrifugation and suggest that LRP1 is at least partially localized in lipid rafts in PC12 and N2a cells.

3.2. Lipid raft disruption blocks LRP1 cell-signaling

Methyl-β-cyclodextrin (MβCD) is a cholesterol sequestration reagent known to disrupt lipid rafts (Christian et al., 1997; Edidin, 2003). Unlike other cholesterol-binding agents that incorporate into membranes, cyclodextrins act strictly at the cell-surface, extracting membrane cholesterol. When added at low concentrations or for short periods of time, MβCD may selectively extract cholesterol from lipid rafts and thereby disrupt the structure of these membrane microdomains, while having less effects on other membrane regions (Zidovetzki and Levitan, 2007).

Fig. 2A shows that in PC12 and N2a cells treated with 1 mM MβCD for 30 min, the amount of biotinylated LRP1 associated with the Triton X100-insoluble membrane fraction decreased substantially, indicating loss of lipid raft-associated LRP1. Fig. 2B shows that, in control PC12 cells that were not treated with MβCD, the LRP1 ligand, EI-tPA (12 nM), activated ERK1/2, as anticipated (Mantuano et al., 2013; Shi et al., 2009). We studied EI-tPA, as opposed to active tPA, to avoid off-target effects related to the protease activity of

this protein. ERK1/2 activation in response to EI-tPA was blocked by the LRP1 antagonist RAP, suggesting an essential role for LRP1 (Gonias and Campana, 2014; Herz and Strickland, 2001). ERK1/2 activation also was blocked by treating the cells with 1 mM MβCD for 30 min.

Equivalent results were obtained when we studied a second LRP1 ligand, α_2M*, which activated ERK1/2 in PC12 cells only when the cells were not pre-treated with MβCD (Fig. 2C). Figs. 2D and 2E show that *LRP1* gene-silencing blocked ERK1/2 activation in response to EI-tPA and α_2M*, respectively, confirming the role of LRP1. In cells transfected with NTC siRNA, EI-tPA and α_2M* activated ERK1/2 and the response was blocked by MβCD.

Next, we studied the effects of MβCD on LRP1 signaling in N2a cells. ERK1/2 was activated by EI-tPA (Fig. 2F) and α_2M* (Fig. 2G) in N2a cells, in the absence of MβCD, as anticipated (Mantuano et al., 2013; Shi et al., 2009). The response to EI-tPA and α_2M* was blocked by RAP and by pre-treating the cells with 1 mM MβCD. The effects of MβCD on LRP1-initiated cell-signaling in PC12 and N2a cells suggest that localization of LRP1 to lipid rafts may be essential for cell-signaling.

To further test whether lipid raft disruption inhibits LRP1-initiated cell-signaling, we treated PC12 cells with Fumonisin B1 (25 μM) for 24 h. Fumonisin B1 blocks the synthesis of sphingolipids that are key components of lipid rafts (Merrill et al., 1993). Fumonisin B1 blocked ERK1/2 activation in response to 12 nM EI-tPA (Fig. 3A) and 10 nM α_2M* (Fig. 3B).

Trk receptors are essential downstream mediators in the pathway by which LRP1-initiated cell-signaling activates ERK1/2 in neurons and neuron-like cell lines (Shi et al., 2009; Yoon et al., 2013). Because Trk receptors localize to lipid rafts and function in a manner that requires lipid raft integrity (Tsui-Pierchala et al., 2002), we conducted experiments to determine whether activation of SFKs by LRP1 ligands is inhibited by MβCD. SFKs function upstream of Trk receptors in response to LRP1 ligands and are responsible for Trk transactivation (Shi et al., 2009). Fig. 3C shows that SFKs were phosphorylated in PC12 cells treated with EI-tPA or α_2M*. SFK phosphorylation by EI-tPA and α_2M* was blocked when the cells were pre-treated with MβCD.

3.3. Ligand binding and endocytosis by LRP1 do not require lipid rafts

We performed experiments to confirm that MβCD does not affect cell viability. Fig. 4A shows that when PC12 cells were cultured for 24 h in serum-free medium (SFM) with 1 mM MβCD, the viable cell count was not significantly decreased compared with cells cultured in the absence of MβCD. In control cells that were not treated with MβCD, α_2M* significantly promoted cell growth, as did 10% fetal bovine serum (FBS). The effects of α_2M* on PC12 cell growth were blocked by MβCD, suggesting that cell growth is linked to the cell-signaling activity of LRP1.

Next, we studied binding of radio-iodinated α_2M* to PC12 cells at 4° C. We selected α_2M* because unlike other LRP1 ligands, α_2M* binds with high specificity to LRP1 (Strickland et al., 1990). Cells were pre-treated with 1 mM MβCD or with vehicle for 30 min and then

chilled to 4° C. Different concentrations of ^{125}I-α_2M* were added to the wells. Binding was allowed to reach equilibrium over 4 h at 4° C, a time pre-determined to be sufficient, as previously described (Hussaini et al., 1990; LaMarre et al., 1993). In some wells, a 100-fold molar excess of unlabeled α_2M* was added to displace specifically bound ^{125}I-α_2M*. Fig. 4B shows that pre-treating cells with MβCD did not significantly affect specific binding of ^{125}I-α_2M* to PC12 cells. In cells that were pre-treated with vehicle, the K_D for α_2M*-binding to PC12 cells was 3.7±1.0 nM (n=3). The B_{max}, which reports the total number of α_2M* binding sites, was 75±7 fmol/mg cell protein. Assuming an average cell mass of about 1 ng, the B_{max} corresponds to 4.5×10^4 α_2M*-binding sites per PC12 cell. In cells that were pre-treated with MβCD, the K_D for α_2M*-binding was 3.6±0.8 nM and the B_{max} was 67±5 fmol/mg cell protein (differences not statistically significant by Student's t-test).

We also studied endocytosis of ^{125}I-α_2M* by PC12 cells at 37° C. Cells were pre-treated with 1 mM MβCD or vehicle for 30 min, washed, and re-equilibrated in DMEM with 5 nM ^{125}I-α_2M* and 1.0 mg/ml BSA at 37° C, in the presence and absence of unlabeled α_2M*. Because the MβCD was washed out before adding α_2M*, control studies were performed to confirm that the distribution of LRP1 between lipid rafts and non-raft membrane fractions did not revert during the subsequent 80 min incubation at 37° C. Fig. 4C shows that MβCD decreased the fraction of LRP1 associated with the detergent-insoluble membrane fraction in PC12 cells, as shown in Fig. 2A. When the cultures were washed and the cells incubated in the absence of MβCD for up to 80 min at 37° C, the amount of LRP1 associated with the detergent-insoluble membrane fraction remained unchanged or continued to decrease. We concluded that LRP1 remained excluded from lipid raft-like membrane microdomains throughout the endocytosis experiment.

Fig. 4D shows that pre-treating PC12 cells with MβCD did not decrease the capacity of the cells to internalize α_2M*. Thus, LRP1 depletion from lipid rafts is not associated with a decrease in the endocytic activity of LRP1.

3.4. Lipid raft disruption blocks LRP1-mediated neurite outgrowth

In neurons and neuron-like cells, Trk receptor transactivation downstream of LRP1 promotes neurite outgrowth (Mantuano et al., 2008; Shi et al., 2009; Yoon et al., 2013). Neurite outgrowth is thus, an LRP1 signal transduction-dependent event. We cultured PC12 cells in the presence or absence of 1 mM MβCD and then treated the cells with 12 nM EI-tPA, 10 nM α_2M*, or vehicle for 48 h. As shown in representative images (Fig. 5A), EI-tPA and α_2M* stimulated neurite outgrowth and this activity was blocked by MβCD.

Images collected in three separate experiments were subjected to image analysis. The results are summarized in Fig. 5B. EI-tPA and α_2M* stimulated neurite outgrowth in PC12 cells by nearly 4-fold. The activity of EI-tPA and α_2M* was blocked by RAP, suggesting an essential role for LRP1. The activity of EI-tPA and α_2M* also was substantially inhibited by MβCD.

Next, we examined primary cultures of CGNs. The CGNs were pre-treated with 1 mM MβCD or vehicle for 30 min and then stimulated with 12 nM EI-tPA or 10 nM α_2M* for 10 min. ERK1/2 activation was examined by immunofluorescence (IF) microscopy using an antibody that detects the phosphorylated forms of ERK1 and ERK2. As shown in Fig. 6,

control CGNs demonstrated robust responses to EI-tPA and α_2M*. Numerous cells were phospho-ERK1/2-immunopositive. When the CGNs were pre-treated with MβCD, ERK1/2 activation in response to EI-tPA and α_2M* was blocked.

EI-tPA and α_2M* stimulated neurite outgrowth in CGNs (Fig. 7), as previously reported (Shi et al., 2009). When the CGNs were treated with MβCD, neurite outgrowth in response to EI-tPA and α_2M* was significantly inhibited. We conclude that lipid raft-like plasma membrane microdomains are important in the function of LRP1 in neurons, both in signal transduction and in neurite outgrowth.

4. Discussion

Lipid rafts and other plasma membrane microdomains allow for specialized membrane functions that support cell physiology (Brown and London, 1998, 2000). In neurons, lipid rafts have been implicated in the assembly of proteins involved in neurotransmitter signaling (Tsui-Pierchala et al., 2002). Rafts facilitate transport of neurotransmitters to the axon terminal, regulate exocytosis of neurotransmitters at the synapse, and organize neurotransmitter receptors and associated signal transduction molecules. Rafts are abundant in dendritic spines (Hering et al., 2003). This is also a location where LRP1 is concentrated in association with proteins such as the NMDA-R and PSD-95 (Brown et al., 1997; May et al., 2004). When PC12 or N2a cells are treated with EI-tPA or α_2M*, LRP1 forms a complex with PSD-95 and the NMDA-R (Mantuano et al., 2013). This complex is essential for transactivation of Trk receptors, ERK1/2 activation, and biological responses such as neurite outgrowth (Bacskai et al., 2000; Mantuano et al., 2013).

We initiated the current study to understand why LRP1 may function as a cell-signaling receptor selectively in specific cell-types (Gonias and Campana, 2014). Our previous studies suggested that the fractional distribution of LRP1 into lipid rafts may be cell type-specific (Wu and Gonias, 2005). Herein, we demonstrate that substantial amounts of LRP1 are raft-associated in PC12 cells and N2a cells. These are cells in which robust LRP1-initiated cell-signaling responses are observed (Mantuano et al., 2013; Mantuano et al., 2008; Shi et al., 2009). Substantially less LRP1 was associated with lipid rafts in VSMCs and CHO cells, confirming our previous results (Wu and Gonias, 2005). Localization of LRP1 to lipid rafts in PC12 and N2a cells may reflect the activity of PSD-95, which is known to cluster other membrane proteins in rafts through its scaffolding activity (Hering et al., 2003; Wong and Schlichter, 2004; Yoshii and Constantine-Paton, 2007).

Using two distinct methods for disrupting lipid rafts, we demonstrated that rafts may be essential for LRP1-initiated cell-signaling in PC12 and N2a cells. Lipid raft disruption failed to affect the total ligand-binding capacity of LRP1, indicating that the number of copies of LRP1 at the cell surface was unchanged. The binding affinity for α_2M* also was unchanged. Furthermore, when raft-associated LRP1 was depleted by pre-treating the cells with MβCD, the endocytic activity of LRP1 remained largely intact. These results suggest that raft disruption selectively affects the signaling activity of LRP1 without affecting other LRP1 activities.

Whether the lower level of raft-associated LRP1 in VSMCs and CHO cells precludes LRP1 signaling remains to be determined. LRP1-signaling in VSMCs is particularly important given the function of VSMC LRP1 in aneurysm prevention (Strickland et al., 2014). In neurons, the NMDA-R is known to traffic in and out of lipid rafts (Delint-Ramirez et al., 2010). It is therefore plausible that rafts are essential for LRP1 signaling selectively in neurons and neuron-like cells because, in these cells, rafts facilitate formation of LRP1-NMDA-R complexes (Mantuano et al., 2013). The NMDA-R also has been identified as an essential LRP1 co-receptor in Schwann cells (Mantuano et al., 2015). Whether the NMDA-R functions in LRP1 signaling in other cell types remains to be determined.

Rodal et al (Rodal et al., 1999) reported that MβCD decreases the capacity of Hep-2 cells to mediate endocytosis of transferrin by as much as 40%. This observation highlights the caveat that MβCD may affect the structure and function of membrane microdomains in addition to lipid rafts (Zidovetzki and Levitan, 2007). Like LRP1, transferrin undergoes endocytosis in clathrin-coated pits (Harding et al., 1983). In our studies, we used a low concentration of MβCD and short exposure time because these conditions limit cholesterol depletion from non-raft membrane fractions (Zidovetzki and Levitan, 2007). Thus, our conditions may explain why the function of LRP1 in ligand-binding and endocytosis was not affected by MβCD. Also, our MβCD wash-out method may have precluded observing minor changes in the function of coated pits in endocytosis of α_2M^*-LRP1 complex. We conclude that the effects of MβCD on LRP1 signaling and endocytic activity are distinct. The former is dependent on lipid raft integrity whereas the latter is not.

LRP1 in lipid rafts is not a static receptor sub-population (Wu and Gonias, 2005). Instead, the distribution of LRP1 in the plasma membrane is dynamic. We previously demonstrated that LRP1 resides transiently in rafts and transfers to clathrin-coated pits, where it undergoes endocytosis (Wu and Gonias, 2005). Once clathrin-coated endosomes invaginate, LRP1 enters an intracellular vesicular transport pathway, disallowing LRP1 transfer back to lipid rafts. Ligands that are internalized with LRP1 are transported to lysosomes. The LRP1 recycles back to the cell surface with nearly 100% efficiency (Dickson et al., 1981; Van Leuven et al., 1980; Willingham et al., 1980).

In PC12 cells and in CGNs, EI-tPA or α_2M^* stimulated neurite outgrowth and this response was blocked by MβCD. ERK1/2 activation in CGNs also was blocked by MβCD. SFK activation and Trk transactivation are essential in the pathway by which LRP1 ligands stimulate ERK1/2 activation and neurite outgrowth (Shi et al., 2009). The inability of EI-tPA or α_2M^* to promote neurite outgrowth in MβCD-treated cells reflected the effects of MβCD on LRP1-signaling. We did not test whether MβCD regulates Trk receptor function, independently of LRP1; however, the effects of MβCD on SFK activation confirmed that depletion of LRP1 from lipid rafts is sufficient to deactivate the pathway by which LRP1 ligands induce neurite outgrowth.

For the first time, we report that α_2M^* may function to promote PC12 cell proliferation. This result is consistent with the demonstrated effects of α_2M^* on cell signaling in this cell line. The effects of α_2M^* on PC12 cell proliferation were blocked by MβCD. Thus PC12 cell proliferation, like neurite outgrowth, probably requires LRP1 localization to lipid rafts.

We believe that LRP1-dependent cell-signaling initiated in lipid rafts may play a major role in the response of neurons to central nervous system injury.

5. Conclusions

Overall, this work demonstrates that the multifunctional nature of LRP1 requires its localization to distinct plasma membrane microdomains. LRP1 partitioning in the plasma membrane may allow for differential regulation of cell-signaling and endocytic activity.

Acknowledgments

References

Allen JA, Halverson-Tamboli RA, Rasenick MM. Lipid raft microdomains and neurotransmitter signalling. Nat Rev Neurosci. 2007; 8:128–140. [PubMed: 17195035]

Bacskai BJ, Xia MQ, Strickland DK, Rebeck GW, Hyman BT. The endocytic receptor protein LRP also mediates neuronal calcium signaling via N-methyl-D-aspartate receptors. Proc Natl Acad Sci U S A. 2000; 97:11551–11556. [PubMed: 11016955]

Barker TH, Pallero MA, MacEwen MW, Tilden SG, Woods A, Murphy-Ullrich JE, Hagood JS. Thrombospondin-1-induced focal adhesion disassembly in fibroblasts requires Thy-1 surface expression, lipid raft integrity, and Src activation. J Biol Chem. 2004; 279:23510–23516. [PubMed: 15033989]

Boucher P, Liu P, Gotthardt M, Hiesberger T, Anderson RG, Herz J. Platelet-derived growth factor mediates tyrosine phosphorylation of the cytoplasmic domain of the low Density lipoprotein receptor-related protein in caveolae. J Biol Chem. 2002; 277:15507–15513. [PubMed: 11854295]

Brown DA, London E. Functions of lipid rafts in biological membranes. Annu Rev Cell Dev Biol. 1998; 14:111–136. [PubMed: 9891780]

Brown DA, London E. Structure and function of sphingolipid- and cholesterol-rich membrane rafts. J Biol Chem. 2000; 275:17221–17224. [PubMed: 10770957]

Brown DA, Rose JK. Sorting of GPI-anchored proteins to glycolipid-enriched membrane subdomains during transport to the apical cell surface. Cell. 1992; 68:533–544. [PubMed: 1531449]

Brown MD, Banker GA, Hussaini IM, Gonias SL, VandenBerg SR. Low density lipoprotein receptor-related protein is expressed early and becomes restricted to a somatodendritic domain during neuronal differentiation in culture. Brain Res. 1997; 747:313–317. [PubMed: 9046007]

Christian AE, Haynes MP, Phillips MC, Rothblat GH. Use of cyclodextrins for manipulating cellular cholesterol content. J Lipid Res. 1997; 38:2264–2272. [PubMed: 9392424]

Cohen AW, Hnasko R, Schubert W, Lisanti MP. Role of caveolae and caveolins in health and disease. Physiol Rev. 2004; 84:1341–1379. [PubMed: 15383654]

Cordy JM, Hooper NM, Turner AJ. The involvement of lipid rafts in Alzheimer's disease. Mol Membr Biol. 2006; 23:111–122. [PubMed: 16611586]

Delint-Ramirez I, Fernández E, Bayés A, Kicsi E, Komiyama NH, Grant SG. In vivo composition of NMDA receptor signaling complexes differs between membrane subdomains and is modulated by PSD-95 and PSD-93. J Neurosci. 2010; 30:8162–8170. [PubMed: 20554866]

Dickson RB, Nicolas JC, Willingham MC, Pastan I. Internalization of alpha 2 macroglobulin in receptosomes. Studies with monovalent electron microscopic markers. Exp Cell Res. 1981; 132:488–493. [PubMed: 6163650]

Edidin M. The state of lipid rafts: from model membranes to cells. Annu Rev Biophys Biomol Struct. 2003; 32:257–283. [PubMed: 12543707]

Fuentealba RA, Liu Q, Kanekiyo T, Zhang J, Bu G. Low density lipoprotein receptor-related protein 1 promotes anti-apoptotic signaling in neurons by activating Akt survival pathway. J Biol Chem. 2009; 284:34045–34053. [PubMed: 19815552]

Goldstein JL, Anderson RG, Brown MS. Coated pits, coated vesicles, and receptor-mediated endocytosis. Nature. 1979; 279:679–685. [PubMed: 221835]

Goldstein JL, Brown MS, Anderson RG, Russell DW, Schneider WJ. Receptor-mediated endocytosis: concepts emerging from the LDL receptor system. Annu Rev Cell Biol. 1985; 1:1–39. [PubMed: 2881559]

Gonias SL, Campana WM. LDL receptor-related protein-1: a regulator of inflammation in atherosclerosis, cancer, and injury to the nervous system. Am J Pathol. 2014; 184:18–27. [PubMed: 24128688]

Harding C, Heuser J, Stahl P. Receptor-mediated endocytosis of transferrin and recycling of the transferrin receptor in rat reticulocytes. J Cell Biol. 1983; 97:329–339. [PubMed: 6309857]

Hayashi H, Campenot RB, Vance DE, Vance JE. Apolipoprotein E-containing lipoproteins protect neurons from apoptosis via a signaling pathway involving low-density lipoprotein receptor-related protein-1. J Neurosci. 2007; 27:1933–1941. [PubMed: 17314289]

Hering H, Lin CC, Sheng M. Lipid rafts in the maintenance of synapses, dendritic spines, and surface AMPA receptor stability. J Neurosci. 2003; 23:3262–3271. [PubMed: 12716933]

Herz J, Strickland DK. LRP: a multifunctional scavenger and signaling receptor. J Clin Invest. 2001; 108:779–784. [PubMed: 11560943]

Hussaini IM, Srikumar K, Quesenberry PJ, Gonias SL. Colony-stimulating factor-1 modulates alpha 2-macroglobulin receptor expression in murine bone marrow macrophages. J Biol Chem. 1990; 265:19441–19446. [PubMed: 1700978]

Imber MJ, Pizzo SV. Clearance and binding of two electrophoretic "fast" forms of human alpha 2-macroglobulin. J Biol Chem. 1981; 256:8134–8139. [PubMed: 6167573]

LaMarre J, Wolf BB, Kittler EL, Quesenberry PJ, Gonias SL. Regulation of macrophage alpha 2-macroglobulin receptor/low density lipoprotein receptor-related protein by lipopolysaccharide and interferon-gamma. J Clin Invest. 1993; 91:1219–1224. [PubMed: 7680664]

Landowski LM, Pavez M, Brown LS, Gasperini R, Taylor BV, West AK, Foa L. Low-density Lipoprotein Receptor-related Proteins in a Novel Mechanism of Axon Guidance and Peripheral Nerve Regeneration. J Biol Chem. 2016; 291:1092–1102. [PubMed: 26598525]

Li N, Mak A, Richards DP, Naber C, Keller BO, Li L, Shaw AR. Monocyte lipid rafts contain proteins implicated in vesicular trafficking and phagosome formation. Proteomics. 2003; 3:536–548. [PubMed: 12687620]

Li Y, Marzolo MP, van Kerkhof P, Strous GJ, Bu G. The YXXL motif, but not the two NPXY motifs, serves as the dominant endocytosis signal for low density lipoprotein receptor-related protein. J Biol Chem. 2000; 275:17187–17194. [PubMed: 10747918]

Liu Q, Zerbinatti CV, Zhang J, Hoe HS, Wang B, Cole SL, Herz J, Muglia L, Bu G. Amyloid precursor protein regulates brain apolipoprotein E and cholesterol metabolism through lipoprotein receptor LRP1. Neuron. 2007; 56:66–78. [PubMed: 17920016]

Mantuano E, Lam MS, Gonias SL. LRP1 Assembles Unique Co-receptor Systems to Initiate Cell Signaling in Response to Tissue-type Plasminogen Activator and Myelin-associated Glycoprotein. Journal of Biological Chemistry. 2013; 288:34009–34018. [PubMed: 24129569]

Mantuano E, Lam MS, Shibayama M, Campana WM, Gonias SL. The NMDA receptor functions independently and as an LRP1 co-receptor to promote Schwann cell survival and migration. J Cell Sci. 2015; 128:3478–3488. [PubMed: 26272917]

Mantuano E, Mukandala G, Li X, Campana WM, Gonias SL. Molecular dissection of the human alpha(2)-macroglobulin subunit reveals domains with antagonistic activities in cell signaling. Journal of Biological Chemistry. 2008; 283:19904–19911. [PubMed: 18499670]

Matsuo M, Campenot RB, Vance DE, Ueda K, Vance JE. Involvement of low-density lipoprotein receptor-related protein and ABCG1 in stimulation of axonal extension by apoE-containing lipoproteins. Biochim Biophys Acta. 2011; 1811:31–38. [PubMed: 21040802]

May P, Rohlmann A, Bock HH, Zurhove K, Marth JD, Schomburg ED, Noebels JL, Beffert U, Sweatt JD, Weeber EJ, Herz J. Neuronal LRP1 functionally associates with postsynaptic proteins and is

required for normal motor function in mice. Mol Cell Biol. 2004; 24:8872–8883. [PubMed: 15456862]

Merrill AH, van Echten G, Wang E, Sandhoff K. Fumonisin B1 inhibits sphingosine (sphinganine) N-acyltransferase and de novo sphingolipid biosynthesis in cultured neurons in situ. J Biol Chem. 1993; 268:27299–27306. [PubMed: 8262970]

Qiu Z, Hyman BT, Rebeck GW. Apolipoprotein E receptors mediate neurite outgrowth through activation of p44/42 mitogen-activated protein kinase in primary neurons. J Biol Chem. 2004; 279:34948–34956. [PubMed: 15169786]

Rodal SK, Skretting G, Garred O, Vilhardt F, van Deurs B, Sandvig K. Extraction of cholesterol with methyl-beta-cyclodextrin perturbs formation of clathrin-coated endocytic vesicles. Mol Biol Cell. 1999; 10:961–974. [PubMed: 10198050]

Roura S, Cal R, Gálvez-Montón C, Revuelta-Lopez E, Nasarre L, Badimon L, Bayes-Genis A, Llorente-Cortés V. Inverse relationship between raft LRP1 localization and non-raft ERK1,2/ MMP9 activation in idiopathic dilated cardiomyopathy: potential impact in ventricular remodeling. Int J Cardiol. 2014; 176:805–814. [PubMed: 25131918]

Sargiacomo M, Sudol M, Tang Z, Lisanti MP. Signal transducing molecules and glycosyl-phosphatidylinositol-linked proteins form a caveolin-rich insoluble complex in MDCK cells. J Cell Biol. 1993; 122:789–807. [PubMed: 8349730]

Shi Y, Mantuano E, Inoue G, Campana WM, Gonias SL. Ligand Binding to LRP1 Transactivates Trk Receptors by a Src Family Kinase-Dependent Pathway. Science Signaling. 2009; 2

Simons K, Ehehalt R. Cholesterol, lipid rafts, and disease. J Clin Invest. 2002; 110:597–603. [PubMed: 12208858]

Simons K, Toomre D. Lipid rafts and signal transduction. Nat Rev Mol Cell Biol. 2000; 1:31–39. [PubMed: 11413487]

Singer SJ, Nicolson GL. The fluid mosaic model of the structure of cell membranes. Science. 1972; 175:720–731. [PubMed: 4333397]

Strickland DK, Ashcom JD, Williams S, Burgess WH, Migliorini M, Argraves WS. Sequence identity between the alpha 2-macroglobulin receptor and low density lipoprotein receptor-related protein suggests that this molecule is a multifunctional receptor. J Biol Chem. 1990; 265:17401–17404. [PubMed: 1698775]

Strickland DK, Au DT, Cunfer P, Muratoglu SC. Low-density lipoprotein receptor-related protein-1: role in the regulation of vascular integrity. Arterioscler Thromb Vasc Biol. 2014; 34:487–498. [PubMed: 24504736]

Tsui-Pierchala BA, Encinas M, Milbrandt J, Johnson EM. Lipid rafts in neuronal signaling and function. Trends Neurosci. 2002; 25:412–417. [PubMed: 12127758]

Van Leuven F, Cassiman JJ, Van Den Berghe H. Primary amines inhibit recycling of alpha 2M receptors in fibroblasts. Cell. 1980; 20:37–43. [PubMed: 6156003]

Vetrivel KS, Cheng H, Lin W, Sakurai T, Li T, Nukina N, Wong PC, Xu H, Thinakaran G. Association of gamma-secretase with lipid rafts in post- Golgi and endosome membranes. J Biol Chem. 2004; 279:44945–44954. [PubMed: 15322084]

Wang L, Murphy-Ullrich JE, Song Y. Molecular insight into the effect of lipid bilayer environments on thrombospondin-1 and calreticulin interactions. Biochemistry. 2014; 53:6309–6322. [PubMed: 25260145]

Weaver AM, McCabe M, Kim I, Allietta MM, Gonias SL. Epidermal growth factor and platelet-derived growth factor-BB induce a stable increase in the activity of low density lipoprotein receptor-related protein in vascular smooth muscle cells by altering receptor distribution and recycling. J Biol Chem. 1996; 271:24894–24900. [PubMed: 8798766]

Webb DJ, Hussaini IM, Weaver AM, Atkins TL, Chu CT, Pizzo SV, Owens GK, Gonias SL. Activated alpha 2-macroglobulin promotes mitogenesis in rat vascular smooth muscle cells by a mechanism that is independent of growth- factor-carrier activity. Eur J Biochem. 1995; 234:714–722. [PubMed: 8575427]

Williamson R, Thompson AJ, Abu M, Hye A, Usardi A, Lynham S, Anderton BH, Hanger DP. Isolation of detergent resistant microdomains from cultured neurons: detergent dependent alterations in protein composition. BMC Neurosci. 2010; 11:120. [PubMed: 20858284]

Willingham MC, Maxfield FR, Pastan I. Receptor-mediated endocytosis of alpha 2-macroglobulin in cultured fibroblasts. J Histochem Cytochem. 1980; 28:818–823. [PubMed: 6160180]

Wong W, Schlichter LC. Differential recruitment of Kv1.4 and Kv4.2 to lipid rafts by PSD-95. J Biol Chem. 2004; 279:444–452. [PubMed: 14559911]

Wu L, Gonias SL. The low-density lipoprotein receptor-related protein-1 associates transiently with lipid rafts. J Cell Biochem. 2005; 96:1021–1033. [PubMed: 16149055]

Yoon C, Van Niekerk EA, Henry K, Ishikawa T, Orita S, Tuszynski MH, Campana WM. Low-density lipoprotein receptor-related protein 1 (LRP1)-dependent cell signaling promotes axonal regeneration. J Biol Chem. 2013; 288:26557–26568. [PubMed: 23867460]

Yoshii A, Constantine-Paton M. BDNF induces transport of PSD-95 to dendrites through PI3K-AKT signaling after NMDA receptor activation. Nat Neurosci. 2007; 10:702–711. [PubMed: 17515902]

Zhuo M, Holtzman DM, Li Y, Osaka H, DeMaro J, Jacquin M, Bu G. Role of tissue plasminogen activator receptor LRP in hippocampal long-term potentiation. J Neurosci. 2000; 20:542–549. [PubMed: 10632583]

Zidovetzki R, Levitan I. Use of cyclodextrins to manipulate plasma membrane cholesterol content: evidence, misconceptions and control strategies. Biochim Biophys Acta. 2007; 1768:1311–1324. [PubMed: 17493580]

Highlights

- In neuron-like cells, the plasma membrane receptor, LRP1, localizes partially in lipid rafts.

- Lipid rafts are required for LRP1-activated cell-signaling and neurite outgrowth.

- Lipid raft disruption has no effect on ligand-binding to LRP1 or LRP1 endocytic activity.

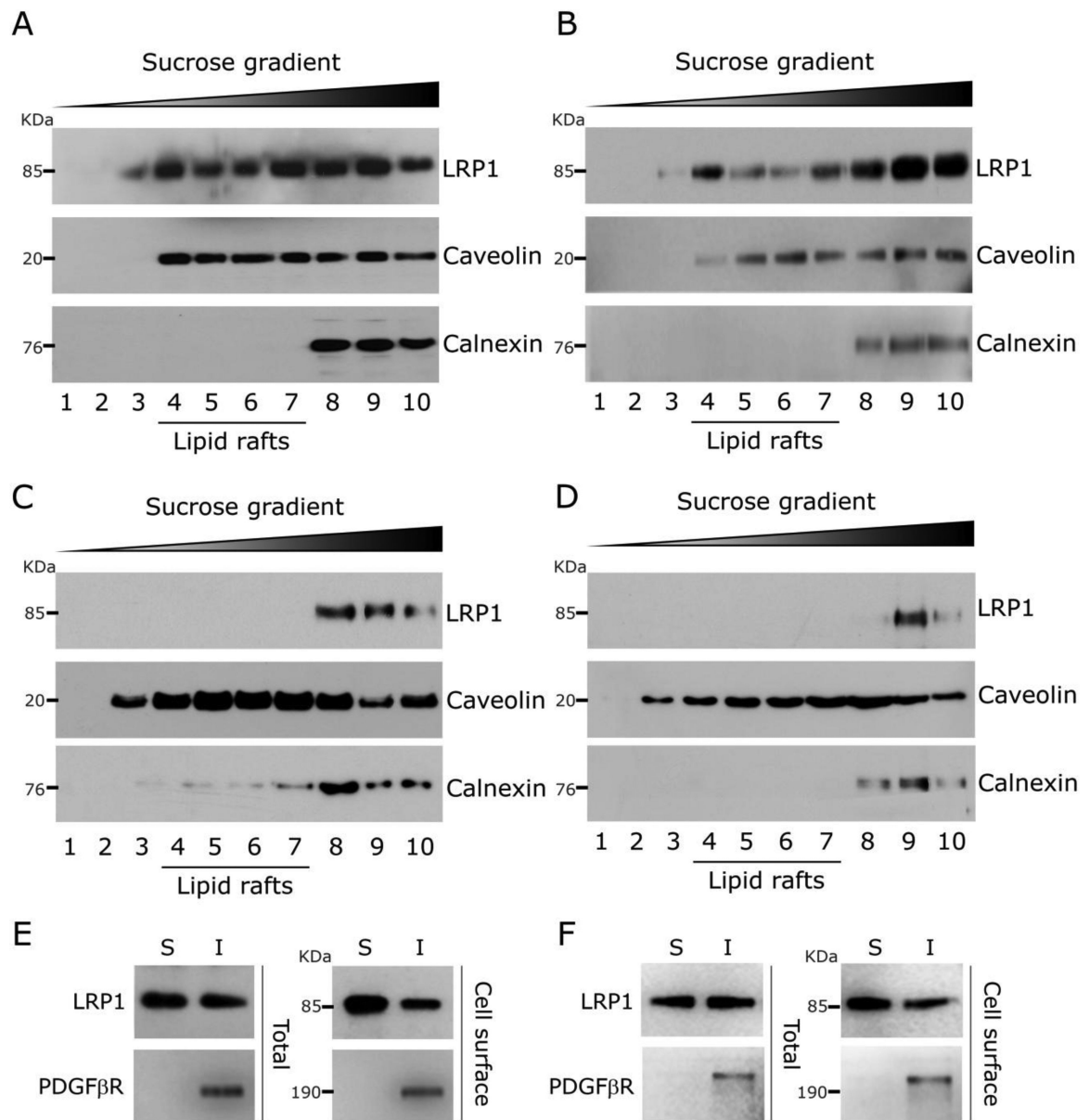- Partitioning of LRP1 in the plasma membrane differentially regulates its activities in neurons.

Fig. 1.
LRP1 distribution into lipid rafts. (A) Homogenates of PC12 cells were prepared in Triton X100. The homogenates were subjected to sucrose density gradient ultracentrifugation. Gradient fractions were numbered in order of increasing density. Immunoblot analysis was performed to detect specific proteins in the fractions. (B) Sucrose density gradient ultracentrifugation analysis of homogenates from N2a cells. (C) Sucrose density gradient ultracentrifugation analysis of VSMCs. (D) Sucrose density gradient ultracentrifugation analysis of CHO-K1 cells. (E) Triton X100 extracts were prepared from PC12 cells in which cell-surface proteins were biotinylated. The detergent soluble "S" and insoluble "I" fractions were subjected to immunoblot analysis to detect LRP1 and PDGFβR (total). The same analysis was performed after affinity-precipitating the fractions to recover biotinylated

proteins (cell-surface). (F) Triton X100 extracts were prepared from N2a cells and analyzed as described in panel E.
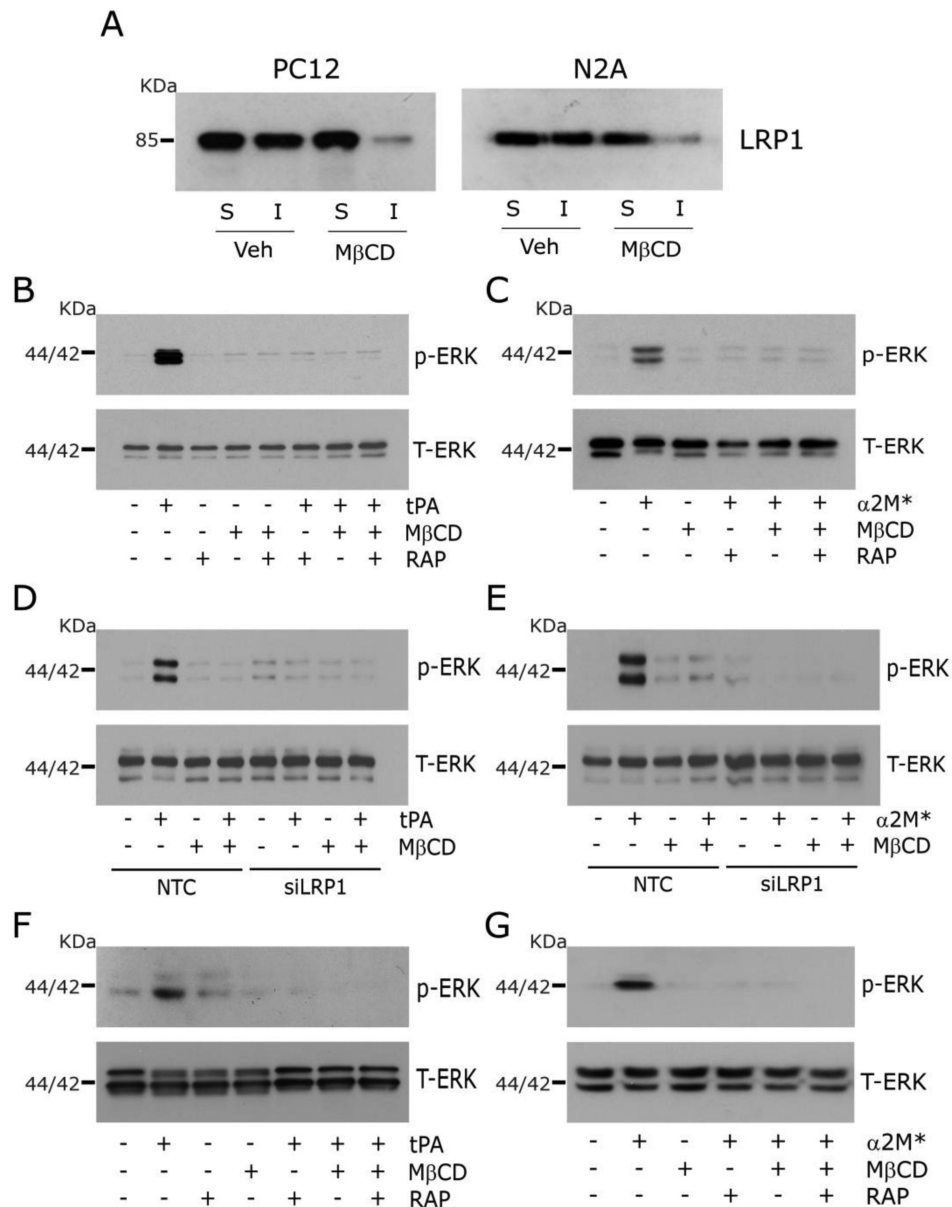
Fig. 2.
Disruption of lipid rafts blocks LRP1 signaling. (A) Immunoblot analysis comparing cell-surface LRP1 in Triton X100-soluble "S" and insoluble "I" fractions from PC12 and N2a cells after pre-treatment for 30 min with MβCD (1 mM) or vehicle. Cell-surface proteins were obtained by affinity precipitation after biotin-labeling. (B) PC12 cells were pre-treated with MβCD (+) or vehicle (−) for 30 min, and then with 150 nm RAP (+) or vehicle (−) for 30 min, followed by 12 nM EI-tPA (+) or vehicle (−) for 10 min. Immunoblot analysis was performed for phospho-ERK1/2 and total ERK1/2. (C) The study described in panel B was repeated, substituting α₂M* (10 nM) for EI-tPA. (D) PC12 cells were transfected with LRP1-specific or NTC siRNA. The cells were treated with 1 mM MβCD (+) or vehicle (−) for 30 min, and then with EI-tPA (12 nM) or vehicle. (E) The study described in panel D

was repeated, substituting α_2M^* (10 nM) for EI-tPA. (F, G) The experiments shown in panels B and C were repeated using N2a cells.
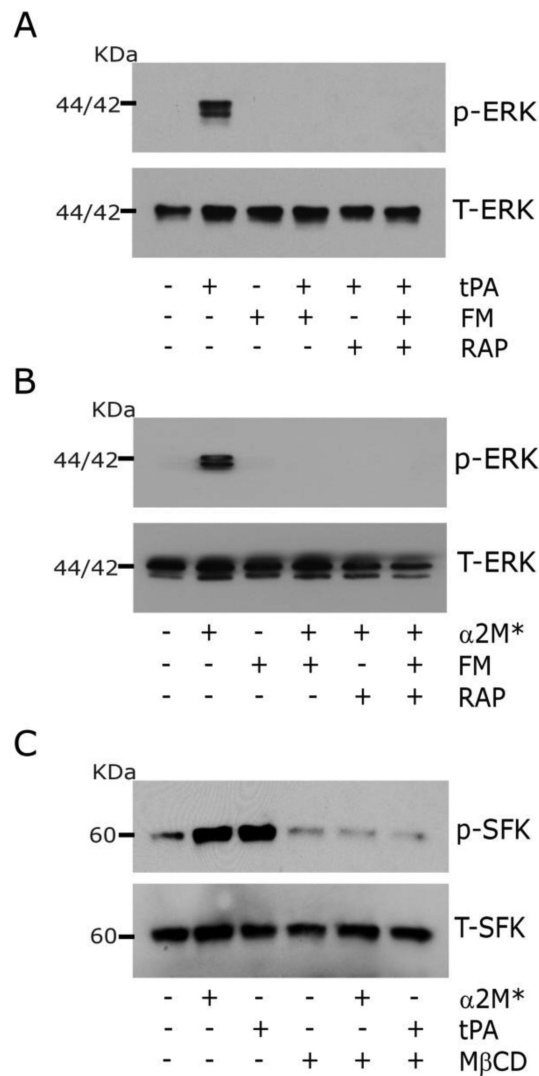
Fig. 3.
Inhibiting synthesis of sphingolipids required for lipid raft formation blocks LRP1 signaling. (A) PC12 cells were treated with 25 μM Fumonisin B1 (FM, +) or with vehicle (FM, −) for 24 h. The cells were then pre-treated with 150 nM RAP (+) or vehicle (−) for 30 min as indicated, followed by EI-tPA (+) or vehicle (−) for 10 min. Phospho-ERK1/2 and total ERK1/2 were determined by immunoblot analysis. (B) The experiment described in panel A was repeated. $\alpha_2 M^*$ (10 nM) was substituted for EI-tPA. (C) PC12 cells were pre-treated with 1 mM MβCD (+) or vehicle (−) for 30 min. The cells were then treated with 12 nM EI-tPA, 10 nM $\alpha_2 M^*$, or vehicle. Immunoblot analysis was performed to detect phosphorylated Src family kinases and total levels of SFK.
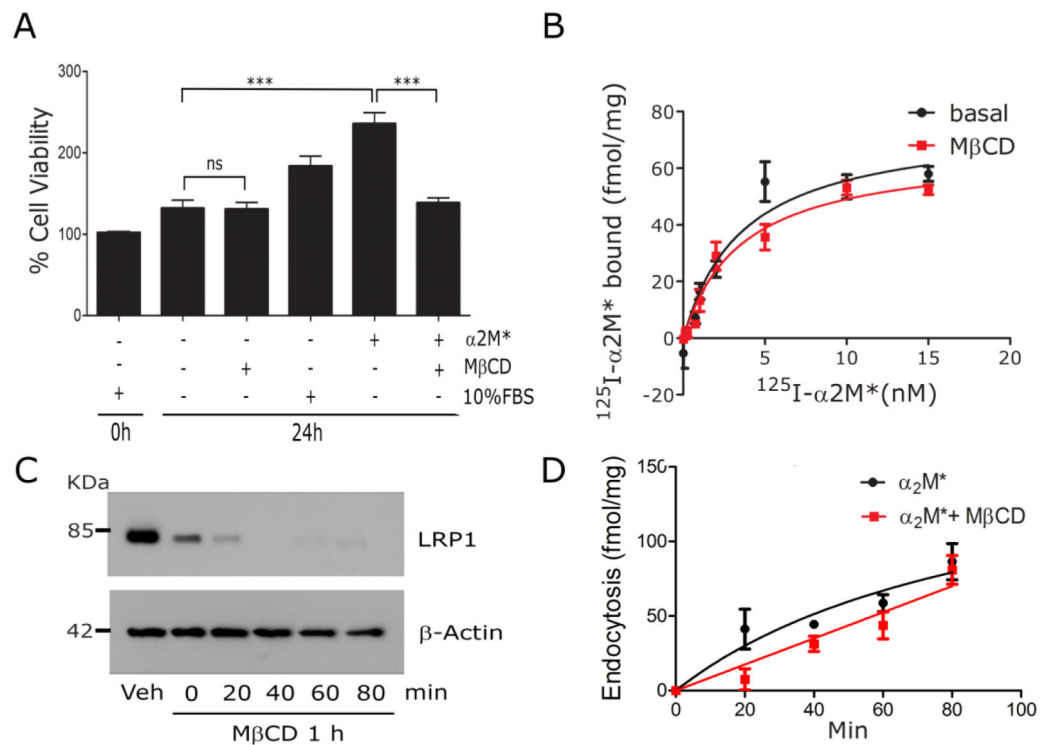
Fig. 4.
The ligand-binding and endocytic activity of LRP1 are unchanged by lipid raft disruption.
(A) PC12 cells were cultured in SFM with 1 mM MβCD, 10 nM α$_2$M*, or 10% FBS, as indicated. WST-1 cell viability assays were performed (mean ± SEM, ns, not statistically significant, ***p<0.001). (B) PC12 cells were treated with 1 mM MβCD or vehicle (basal) for 30 min and then equilibrated at 4° C. Specific binding of ^{125}I-α$_2$M* was determined. The results of three separate experiments were averaged. (C) PC12 cells were surface-labeled with biotin and then treated with 1 mM MβCD or vehicle for 30 min. The cultures were washed and the medium replaced with EHB medium (no MβCD) for the indicated times. Detergent-soluble "S" and -insoluble "I" fractions were prepared. Biotinylated proteins in the fractions were affinity-precipitated and LRP1 was detected by immunoblot analysis. Actin in unfractionated extracts was measured as a control for load. (D) PC12 cells were pre-treated with MβCD or vehicle. The cultures were washed and re-established in EHB with 5 nM ^{125}I-α$_2$M*, in the presence and absence of unlabeled α$_2$M*, at 37° C. Internalized radioligand was determined as a function of time. Presented results represent three separate experiments.
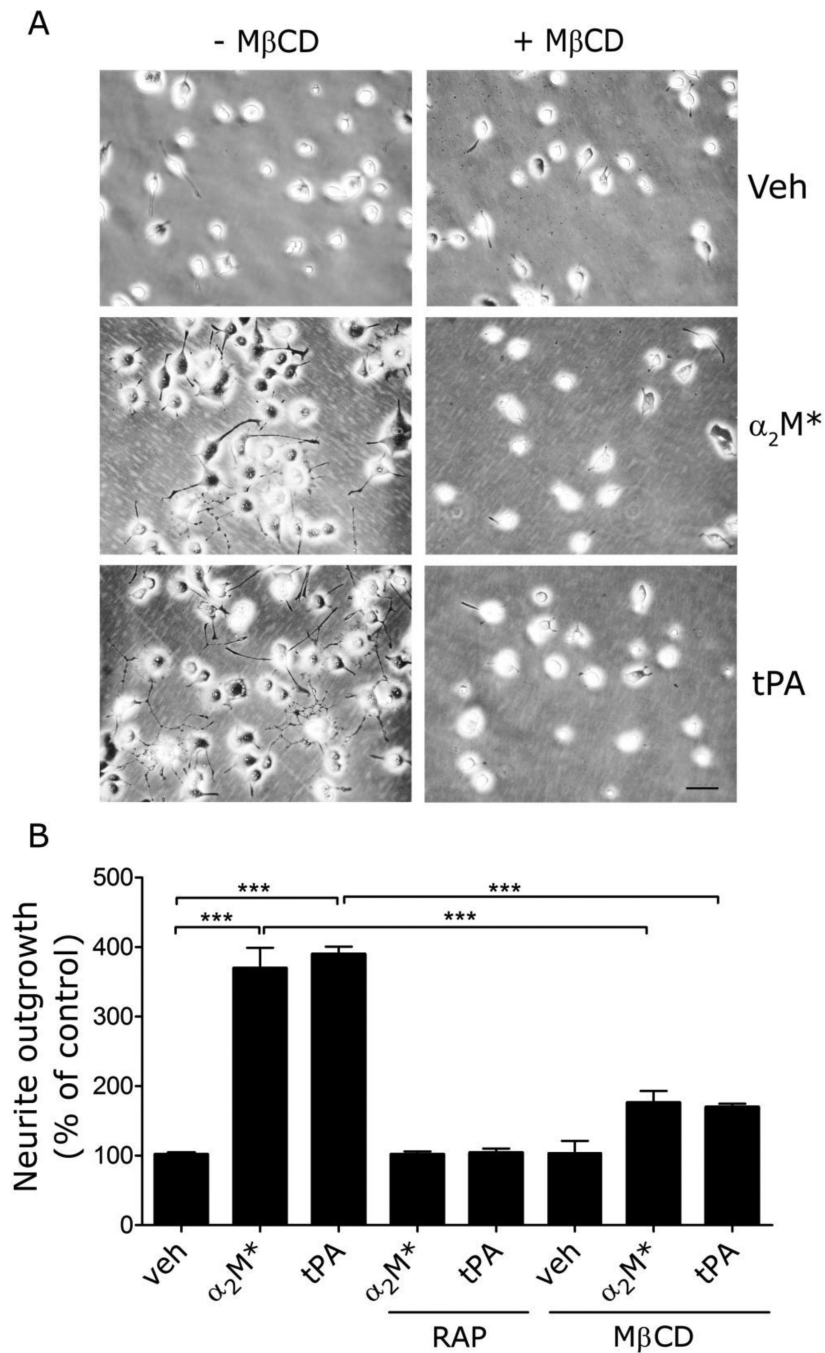
Fig. 5.
Lipid raft disruption blocks the ability of LRP1 ligands to promote neurite outgrowth in PC12 cells. (A) PC12 cells were treated with $\alpha_2 M^*$ (10 nM), EI-tPA (12 nm), or vehicle for 48 h in the presence or absence of 150 nM RAP or 1 mM MβCD. Neurite outgrowth was detected by phase contrast microscopy. Representative images are shown (scale bar, 40 μm). (B) Neurite length was determined for 50 cells, chosen at random, in three different experiments (***p<0.001).
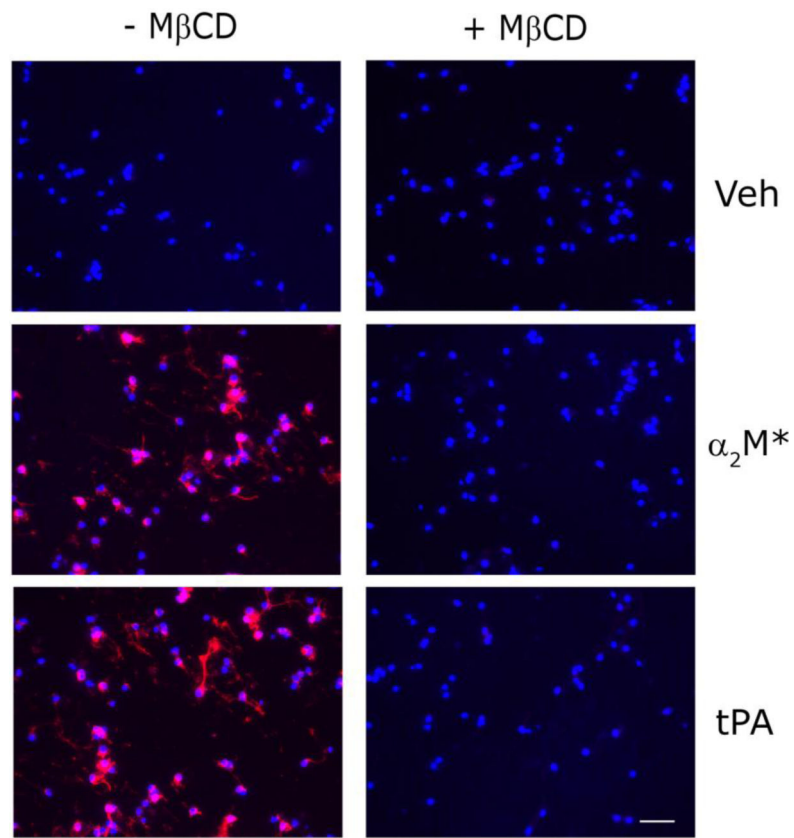
Fig. 6.
Lipid raft disruption blocks LRP1 signaling in neurons. CGNs were pre-treated with 1 mM MβCD or vehicle for 30 min. The cells were then treated with α$_2$M* (10 nm), EI-tPA (12 nm), or vehicle for 10 min. IF microscopy was performed to detect phospho-ERK1/2 (red). Nuclei were stained with DAPI (blue). Merged images are presented (scale bar, 50 μm).
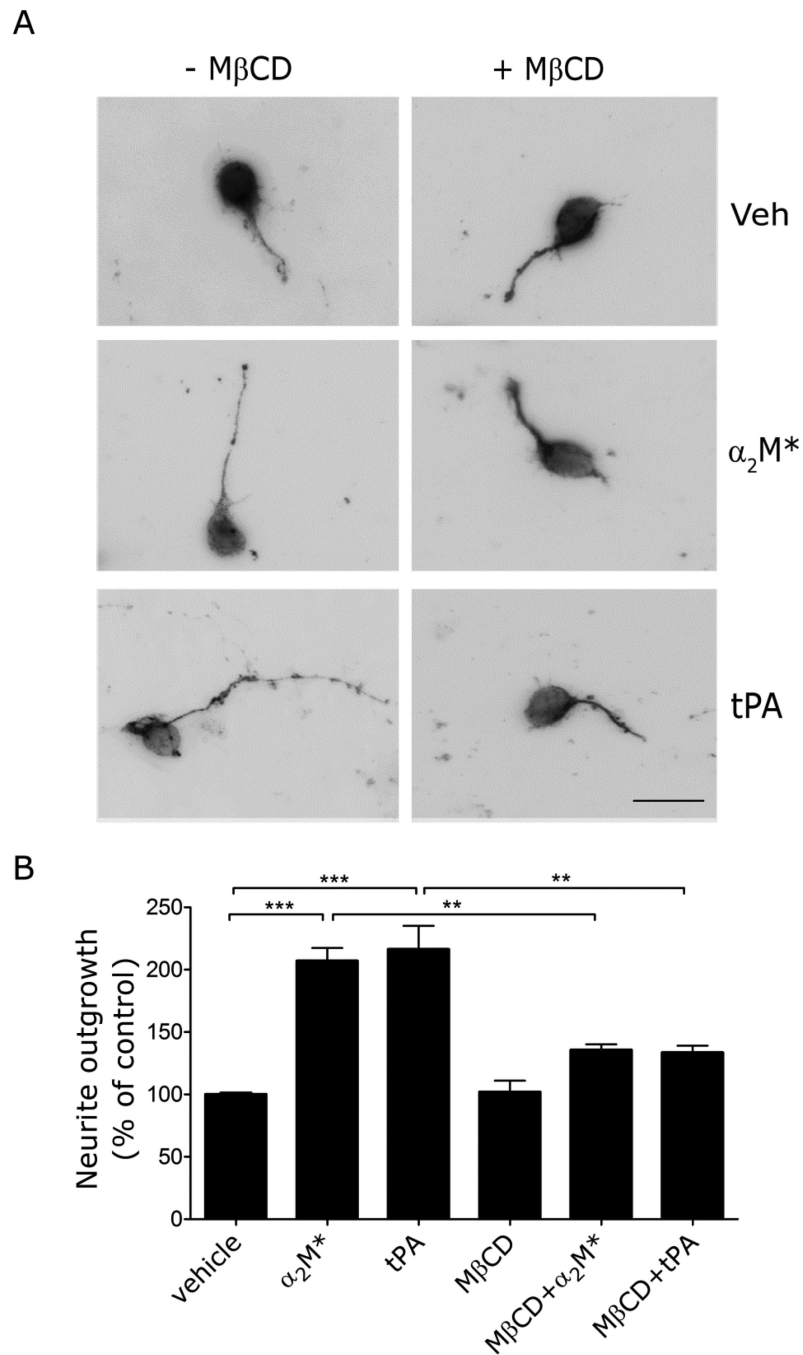
A

B

Fig. 7.
Neurite outgrowth in CGNs is inhibited by lipid raft disruption. (A) CGNs were cultured for 48 h in the presence of the α_2M^* (10 nM), EI-tPA (12 nm) or vehicle, in the presence or absence of MβCD (1 mM). The neurons were immunostained to detect β3-tubulin and imaged by fluorescence microscopy (scale bar, 20 μm). (B) Neurite length was determined for 50 randomly selected CGNs for each condition, in three separate experiments (mean ± SEM, ***, p<0.001).